CELL CYCLE
2021, VOL. 20, NO. 9, 914–926
https://doi.org/10.1080/15384101.2021.1909885

Taylor & Francis
Taylor & Francis Group

RESEARCH PAPER

Circular RNA circ_HECTD1 regulates cell injury after cerebral infarction by miR-27a-3p/FSTL1 axis

Zhenduo Zhang[a], Jinbo He[b], and Baoliang Wang[a]

[a]Department of Encephalopathy Third Ward, The First Affiliated Hospital of Henan University of CM, Zhengzhou, Henan, China; [b]Department of ICU, The First Affiliated Hospital of Henan University of CM, Zhengzhou, Henan, China

ABSTRACT

Cerebral infarction is a common cerebrovascular disease caused by neural cell injury, with high mortality worldwide. Circular RNAs HECT domain E3 ubiquitin-protein ligase 1 (circ_HECTD1) has been reported to be related to the oxygen-glucose deprivation/reperfusion (OGD/R)-caused neuronal damage in cerebral ischemia. This study is designed to explore the role and mechanism of circ_HECTD1 in OGD/R-induced cell injury in cerebral ischemia. Circ_HECTD1, microRNA-27a-3p (miR-27a-3p), and Follistatin-like 1 (FSTL1) level were detected by real-time quantitative polymerase chain reaction (RT-qPCR). The localization of circ_HECTD1 was analyzed by subcellular fractionation assay. Cell proliferative ability and apoptosis were assessed by 5-ethynyl-2 -deoxyuridine (EdU), 3-(4, 5-dimethyl-2-thiazolyl)-2, 5-diphenyl-2-H-tetrazolium bromide (MTT), and flow cytometry assays. The protein levels of proliferating cell nuclear antigen (PCNA), B-cell lymphoma-2 (Bcl-2), Bcl-2 related X protein (Bax), Cleaved poly-ADP-ribose polymerase (PARP), and FSTL1 were examined by western blot assay. The binding relationship between miR-27a-3p and circ_HECTD1 or FSTL1 was predicted by starbase 3.0 then verified by a dual-luciferase reporter assay. Circ_HECTD1 and FSTL1 were highly expressed, and miR-27a-3p was decreased in OGD/R-treated HT22 cells. Moreover, circ_HECTD1 knockdown could boost cell proliferative ability and repress apoptosis in OGD/R-triggered HT22 cells *in vitro*. Mechanical analysis discovered that circ_HECTD1 could regulate FSTL1 expression by sponging miR-27a-3p. Circ_HECTD1 deficiency could mitigate OGD/R-induced HT22 cell damage by modulating the miR-27a-3p/FSTL1 axis, providing a promising therapeutic target for cerebral infarction treatment.

ARTICLE HISTORY
Received 2 February 2021
Revised 23 March 2021
Accepted 25 March 2021

KEYWORDS
Circ_hectd1; miR-27a-3p; fstl1; cerebral infarction; oxygen-glucose deprivation

Introduction

As a common cerebrovascular disease, cerebral infarction, also known as cerebral ischemic stroke, has affected the life quality of patients and brought a heavy burden to the family and society [1,2]. Accounts for 80% of all strokes, cerebral infarction is caused by ischemic necrosis or softening of localized brain tissues due to cerebral blood supply disorders, ischemia, and hypoxia [3], with high disability and mortality [4]. Despite the enormous efforts in the therapeutic strategies, such as thrombolysis and neuroprotective agents, the outcomes of patients with cerebral infarction are still unsatisfactory [5,6]. Currently, many scholars have pointed out that oxygen-glucose deprivation/reperfusion (OGD/R), which destroys cell membrane permeability and ultimately leads to neuronal cell death, can be used to construct in vitro models of cerebral infarction [7–9]. Hence, exploring the mechanism of OGD/R-triggered cell injury is imperative to clarify the pathogenesis of cerebral infarction.

Circular RNAs (circRNAs) represent a distinct group of non-coding transcripts that form covalently closed loops without a 5' cap and 3' polyadenylated tail [10,11]. Interestingly, circRNAs are found to be abundant, evolutionarily conserved, and relatively stable in the cytoplasm, which confers circRNAs with many potential functions, such as serving as microRNAs (miRNAs) sponges [12,13]. In fact, as potential biomarkers, numerous circRNAs expression alterations have an inextricable correlation with various cerebrovascular diseases, including ischemic stroke [14,15]. For example, Wu *et al.* presented that the forced expression of circRNA TLK1 exerted a detrimental role in neuronal injury and neurological deficits after ischemic stroke by sponging

CONTACT Zhenduo Zhang zdzhang001002@163.com

miR-335-3p [16]. Meanwhile, Su *et al.* reported that deficiency of circ_ANRIL could relieve OGD/R-induced human brain cells injury by binding to miR-622, such as apoptosis and inflammatory [17]. An early document suggested that circRNA HECT domain E3 ubiquitin-protein ligase 1 (circ_HECTD1) has been identified as highly specific circRNA and predicted a higher risk of acute ischemic stroke recurrence [18]. Furthermore, circ_HECTD1 silencing was previously validated to attenuate OGD/R-caused neuronal damage in cerebral ischemia [19], implying the vital role of circ_HECTD1 in cerebral ischemia. Yet, the regulatory mechanism of circ_HECTD1 has not been fully elucidated in cerebral ischemia.

Up to now, the competing endogenous RNAs (ceRNAs) hypothesis proposed that circRNAs function as essential regulators in some diseases through sequestering their target miRNAs [20,21]. In this research, our finding displayed that circ_HECTD1 was the enhanced expression in OGD/R-treated HT22 cells, and knockdown of circ_HECTD1 mitigated OGD/R-induced cell injury *in vitro*. Apart from that, we first discovered that circ_HECTD1 could interact with miR-27a-3p. Therefore, the purpose of this article is to tunnel whether circ_HECTD1 could regulate OGD/R-caused cell damage through targeting miR-27a-3p in cerebral ischemia.

Materials and methods

Middle cerebral artery occlusion (MCAO) and animal treatment

Ten-week-old male mice (Vital River Laboratory, Beijing, China) under a specific-pathogen-free environment were introduced in this study, which got the approval of the Animal Ethics Committee of the First Affiliated Hospital of Henan University of CM. In short, the mice were anesthetized with isoflurane, followed by incising the middle clerical skin. After occluding of the middle cerebral artery (MCA) using a heparin-dampened nylon suture for 1 h, the filament was removed for reperfusion. For the sham group, the mice have only isolated the MCA without suture insertion. And then, the mice were deeply anesthetized after reperfusion for 12, 24, and 48 h, followed by an analysis of the removed brains.

Cell culture and oxygen-glucose deprivation/reperfusion (OGD/R) model

Under a humidified atmosphere of 5% CO_2 at 37°C, mouse hippocampal neuronal cell line (HT22, cat. CL-0595, Procell, Wuhan, China) were passaged in Dulbecco's modified Eagle's medium (DMEM; Invitrogen, Carlsbad, CA, USA) supplemented with 10% fetal bovine serum (FBS; Invitrogen) and antibiotics (100 U/mL penicillin, 100 μg/mL streptomycin, PAN Biotech, Aidenbach, Germany). Besides, hippocampal neurons have dopamine nerve terminals that are selectively vulnerable to ischemia. HT22 cell line was an immortalized mouse hippocampus neuronal cell line, which commonly and stably used as a hippocampal neuronal cell model in numerous researches. Therefore, HT22 cells were selected for in vitro study.

For OGD/R cell models, HT22 cells in serum/glucose-free DMEM medium were transferred to a hypoxic chamber with (95% nitrogen and 5% CO_2) for 3 h, followed by reoxygenation for 24 h in the glucose-containing DMEM with 10% FBS under normoxic conditions [22]. Besides, cells without OGD/R treatment were applied as a control.

Real-time quantitative polymerase chain reaction (RT-qPCR)

Based on the supplier's direction of TRIzol reagent (Invitrogen), total RNAs from HT22 cells were isolated, followed by reverse transcription to cDNA using the PrimeScript™ RT Master Mix (TaKaRa, Shiga, Japan, for circRNA and mRNA), and the qScript™ microRNA cDNA synthesis kit (Quanta Bioscience, Gaithersburg, MD, USA, for miRNA). On an ABI 7900 System (Applied Biosystems, Foster City, CA, USA), qRT-PCR was implemented using SYBR Green PCR Kit (TaKaRa). After normalization with GAPDH and U6, the calculation of relative RNA expression was performed by using the $2^{-\Delta\Delta Ct}$ method. The sequences of primers in this assay were in (Table 1).

Table 1. The sequences of primers for RT-qPCR used in this study.

Names	Sequences (5′-3′)
Circ_HECTD1: Forward	CACGTGTTATCAGGGGCCTT
Circ_HECTD1: Reverse	CGCCACCCTTGCTTTTCATC
linear HECTD1: Forward	AGACACGGCTTTTCCTGTGC
linear HECTD1: Reverse	CTGGCTCGCCGTACCAAAC
miR-27a-3p: Forward	TTCACAGTGGCTAAGTTCCGC
miR-27a-3p: Reverse	CTCGCTTCGGCAGCACA
FSTL1: Forward	AGATGCCTGCCTCACTGGAT
FSTL1: Reverse	GCTCATCGCGGTTAGCTTGA
U6: Forward	CGCTTCGGCAGCACATATAC
U6: Reverse	TTCACGAATTTGCGTGTCAT
GAPDH: Forward	GCACCACCAACTGCTTAG
GAPDH: Reverse	GCCATCCACAGTCTTCTG

Subcellular fractionation and Ribonuclease R (RNase R) treatment

For subcellular fractionation assay, HT22 cells were suspended in cytoplasm lysis buffer, followed by centrifugation. 4 min later, the cytoplasmic supernatant was transferred to a fresh RNase-free tube, and the remaining was added nucleus lysis buffer and centrifuged for 10 min. Whereafter, the TRIzol reagent (Invitrogen) was used to acquire the RNAs from cytoplasmic and nuclear extracts, followed by the determination of circ_HECTD1, U6 (nucleus control), and GAPDH (cytoplasm control) by RT-qPCR assay. For RNase R treatment, HT22 cells were treated with or without RNase R (3 U/μg, Epicenter, Madison, WI, USA), followed by incubation for 30 min at 37°C. After purification using an RNeasy MinElute Cleanup Kit (Qiagen, Hilden, Germany), the samples were subjected to RT-qPCR analysis of circ_HECTD1 and liner HECTD1.

Cell transfection

For circ_HECTD1 knockdown, HT22 cells were transfected with 50 nM of circ_HECTD1 small interference RNA (si-circ_HECTD1, RiboBio, Guangzhou, China) or non-targeting siRNA (si-NC, RiboBio). Likewise, 50 nM of miR-27a-3p mimic (miR-27a-3p, RiboBio), miR-27a-3p inhibitor (anti-miR-27a-3p) and their negative controls (miR-NC and anti-miR-NC) were separately transfected into HT22 cells. Follistatin-like 1 (FSTL1) overexpression, the FSTL1 sequence (Accession: NM_0080447.5) was inserted into an empty pcDNA vector (Invitrogen, a negative control) to obtain pcDNA-FSTL1 (FSTL1), followed by transfection into HT22 cells with 200 ng vector. According to the supplier's direction of Lipofectamine 3000 (Invitrogen), all transfection was performed for 48 h in this study.

5-ethynyl-2 -deoxyuridine (EdU) assay

The assessment of HT22 cell proliferation was conducted by EdU assay using a Cell-Light™ EdU Apllo®567 In Vitro Imaging Kit (RiboBio). In general, treated or un-treated HT22 cells (2×10^3 cells/well) were introduced into 96-well plates, followed by incubation with 50 μM EdU for 2 h at 37°C. Following fixation in 4% formaldehyde solution for 30 min, the cells were treated with 0.5% Triton X-100 for 20 min for permeabilization, followed by staining with Apollo and Hoechst. After visualization under a fluorescence microscope (Nikon, Tokyo, Japan), the EdU-positive cells were calculated using the formula: EdU add-in cells/Hoechst-stained cells ×100%.

Cell viability assay

Briefly, treated or un-treated HT22 cells were seeded into 96-well plates, followed by the addition of 20 μL 3-(4, 5-dimethyl-2-thiazolyl)-2, 5-diphenyl-2-H-tetrazolium bromide (MTT, 5 mg/mL, Sigma-Aldrich, St. Louis, MO, USA). After incubation for 4 h at 37°C, 150 μL of dimethyl sulfoxide (DMSO, Sigma-Aldrich) was introduced into each well to dissolve the formed formazan crystals. At length, a microplate reader (Bio-Tek Instruments, Hopkinton, MA, USA) was used to detect the absorbance at 570 nm.

Cell apoptosis assay

In brief, treated or un-treated HT22 cells were harvested and washed with PBS (Invitrogen), followed by re-suspended in binding buffer. After staining with 5 μL Annexin (V-fluorescein isothiocyanate, Bender Med System, Vienna, Austria)) V-FITC/Propidium Iodide (PI, Bender Med System) for 15 min, cell apoptosis rare was analyzed using FACSan flow cytometry (BD Bioscience, Heidelberg, Germany).

Western blot assay

After treatment with RIPA lysis buffer (Beyotime, Shanghai, China), an equal amount of lysate samples were separated by 10% SDS-PAGE, followed by 10% SDS-PAGE and transferring onto PVDF membranes (Millipore, Molsheim, France). After blocking with 5% nonfat milk, the membranes were probed with primary antibodies: Proliferating cell nuclear antigen (PCNA, 1:1000, #13,110, Cell Signaling Technology, Beverly, MA, USA), B-cell lymphoma-2 (Bcl-2, 1:1000, #3498, Cell Signaling Technology), Bcl-2 related X protein (Bax, 1:1000; #14,796, Cell Signaling Technology), Cleaved poly-ADP-ribose polymerase (PARP, 1:1000; #94,885, Cell Signaling Technology), FSTL1 (1:1000, ab223287, Abcam, Cambridge, MA, USA), and GAPDH (1:1000; #5174, Cell Signaling Technology) at 4°C overnight, and incubated with secondary antibody (1:2000; #7074, Cell Signaling Technology) at room temperature for 2 h, followed by detection according to the instruction of ECL detection kit (Invitrogen).

Dual-luciferase reporter assay

According to the analysis of starBase v3.0 (http://starbase.sysu.edu.cn) software, the underlying binding relationship between miR-27a-3p and circ_HECTD1 or FSTL1 was verified by dual-luciferase reporter assay. Generally, the fragment sequence of circ_HECTD1 and FSTL1 3' un-translated region (3'UTR) with the putative binding site of miR-27a-3p constructed and inserted into psiCHECK-2 vector (Promega, Madison, WI, USA), generating circ_HECTD1-WT or FSTL1 3'UTR-WT. Likewise, the corresponding mutant (MUT) fragments of circ_HECTD1 and FSTL1 3'UTR were applied to obtain the reporter vectors circ_HECTD1/FSTL1 3'UTR-MUT. Subsequently, these reporter vectors were transfected into HT22 cells along with miR-27a-3p or miR-NC, referring to the producer's instructions of the Lipofectamine 3000 (Invitrogen).

Statistical analysis

Data in this study was exhibited as a mean ± standard deviation (SD), and analyzed using GraphPad Prism7 (GraphPad Software, La Jolla, CA, USA). Data comparisons were performed by Student's *t*-test for two groups and one-way ANOVA with Tukey's tests for multiple groups. $P< 0.05$ was considered statistically significant.

Results

Circ_HECTD1 expression was upregulated upon OGD/R *in vitro* and *in vivo*

Firstly, to detect the expression level of circ_HECTD1 in the pathophysiology of cerebral ischemia stroke, the MCAO operation-induced reperfusion injury was proved using TTC staining. Results exhibited that the infarct volume and brain-damaged were markedly increased by MCAO operation relative to the sham group (Figure 1a and 1b). Subsequently, we further assessed circ_HECTD1 level in brain tissues following middle cerebral artery occlusion/reperfusion (MCAO/R). As shown in (Figure 1c), the expression level of circ_HECTD1 was promoted after MCAO/R in a time-dependent manner, implying the underlying role in ischemia. Whereafter, we further checked the expression of circ_HECTD1 under ischemia condition *in vitro*. As shown in (Figure 1d), the high expression of circ_HECTD1 was noticed in OGD/R-treated HT22 cells when compared with the control group. Moreover, we further verified that circ_HECTD1 was predominantly located in the cytoplasm of HT22 cells, suggesting the possible post-transcriptional regulatory mechanism of circ_HECTD1 in HT22 cells (Figure 1e). Also, to confirm the circular nature of circ_HECTD1, HT22 cells were treated with or with RNase R. As presented in (Figure 1f), the circular isoform was resistant to RNase R, whereas the linear isoform was notably declined in RNase R-treated HT22 cells. Together, these data suggested that the abnormal expression of circ_HECTD1 might be involved with the cerebral infarction.

Knockdown of Circ_HECTD1 boosted cell proliferation and repressed apoptosis in response to OGD/R treatment

Considering the high expression of circ_HECTD1 in OGD/R-treated HT22 cells, we knocked down

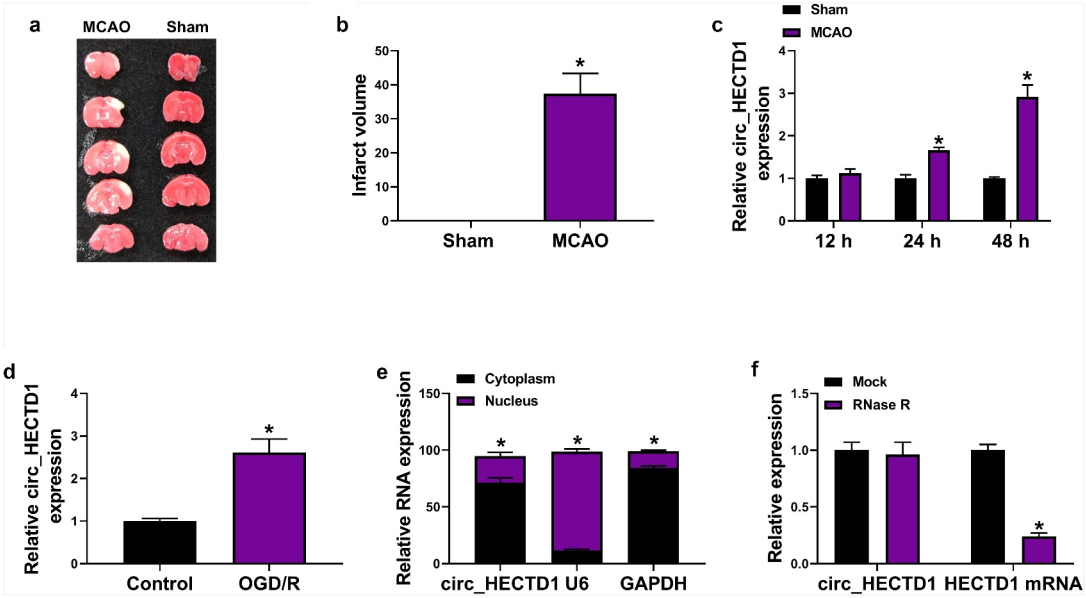

Figure 1. Circ_HECTD1 was increased following OGD/R *in vitro* and *in vivo*. (a) TTC staining assay displayed the representative brain section of focal ischemia induced by MCAO. (b) RT-qPCR assay was applied to analyze the brain infarct volume after I/R in mice. (c) Circ_HECTD1 level was assessed by RT-qPCR assay at 12, 24, and 48 h following MCAO/R in mice. (d)RT-qPCR assay was applied to measure the expression level of circ_HECTD1 in HT22 cells treated with or without OGD/R. (e) The cellular localization of circ_HECTD1 in HT22 cells was analyzed by Subcellular fractionation assay. (f) The levels of circ_HECTD1 and liner HECTD1 mRNA were determined by RT-qPCR assay. *P< 0.05.

circ_HECTD1 in this cell line. As exhibited in (Figure 2a), the introduction of si-circ_HECTD1 reduced the expression level of circ_HECTD1 in HT22 cells, while had no evident effect on liner HECTD1 mRNA, indicating that si-circ_HECTD1 could be employed for the subsequent loss-of-function assays. Then, the EdU incorporation assay analysis displayed that the number of EdU-positive cells was significantly reduced caused by the treatment of OGD/R, while the deficiency of circ_HECTD1 could abolish the effect in HT22 cells (Figure 2b). Consistently, the downregulation of circ_HECTD1 could weaken the repression effect of OGD/R treatment on cell proliferative ability in HT22 cells (Figure 2c). Meanwhile, a proliferation-related marker PCNA was found to be decreased due to the treatment of OGD/R in HT22 cells, which was evidently overturned by circ_HECTD1 deletion (Figure 2d), further supporting the promoting action of circ_HECTD1 knockdown on OGD/R-mediated cell proliferation. Furthermore, enhanced apoptosis rate was observed on account of OGD/R treatment in HT22 cells, whereas the transfection of si-circ_HECTD1 distinctly mitigated the effect (Figure 2e). To further prove the effect, the apoptosis-associated factors (Bcl-2, Bax, and Cleaved PARP) were determined in HT22 cells. As shown in (Figure 2f), the silencing of circ_HECTD1 could abrogate OGD/R-triggered decline in Bcl-2 level, and an increase in Bax and Cleaved PARP levels in HT22 cells. Collectively, these results indicated that circ_HECTD1 deficiency could attenuate OGD/R-caused cell damage in HT22 cells.

Circ_HECTD1 directly interacted with miR-27a-3p

Then, in order to further investigate the mechanism of action of circ_HECTD1, we searched putative circ_HECTD1-interacting miRNAs using the online software starbase3.0. As presented in (Figure 3a), miR-27a-3p was found to have some complementary bases pairing with circ_HECTD1, as proved by a dual-luciferase reporter assay. Data suggested that the luciferase activity in HT22 cells transfected with circ_HECTD1-WT and miR-27a-3p was reduced competed with that in cells with circ_HECTD1-WT and miR-NC, where there was little in the cells transfected with circ_HECTD1-MUT (Figure 3b). Apart from that, we further detected the authentic

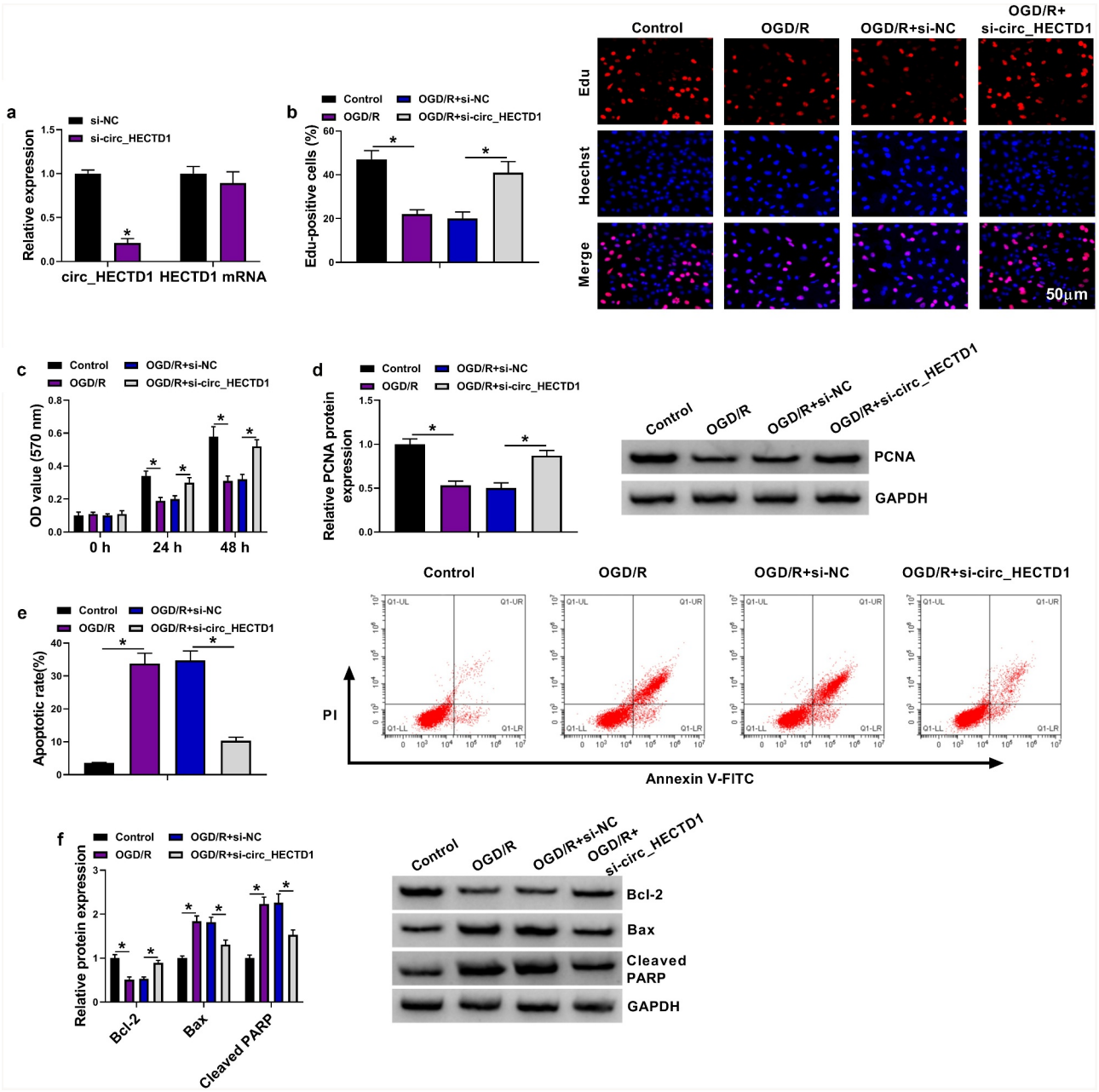

Figure 2. Circ_HECTD1 downregulation promoted cell proliferation and hindered cell apoptosis in OGD/R-induced HT22 cells. (a) The expression levels of circ_HECTD1 and liner HECTD1 mRNA were assessed in si-NC or si-circ_HECTD1-transfected HT22 cells. (b-f) HT22 cells were treated with Control, OGD/R, OGD/R+ si-NC, OGD/R+ si-circ_HECTD1. (b) Cell proliferation was analyzed by EdU assay in treated HT22 cells. (c) Cell viability was detected by MTT assay in treated HT22 cells. (d) PCNA protein level was measured by western blot assay in treated HT22 cells. (e) Apoptosis rate was examined by flow cytometry assay in treated HT22 cells. (f) The protein levels of Bcl-2, Bax, and Cleaved PARP were tested western blot assay in treated HT22 cells. *$P< 0.05$.

impact of circ_HECTD1 on miR-27a-3p in HT22 cells. Results exhibited that the expression level of miR-27a-3p was upregulated in HT22 cells transfected with si-circ_HECTD1 relative to cells transfected with si-NC (Figure 3c). Besides, we further examined miR-27a-3p level in ischemia-induced cerebral injury *in vivo*. As presented in (Figure 3d), miR-27a-3p was apparently declined in a time-dependent manner after reperfusion at 12, 24, and 48 h followed MCAO operation in mice, suggesting the possible role of miR-27a-3p in ischemia. Moreover, our data also verified that the downregulation of miR-27a-3p in HT22 cells after the treatment of OGD/R was noticed in comparison with the

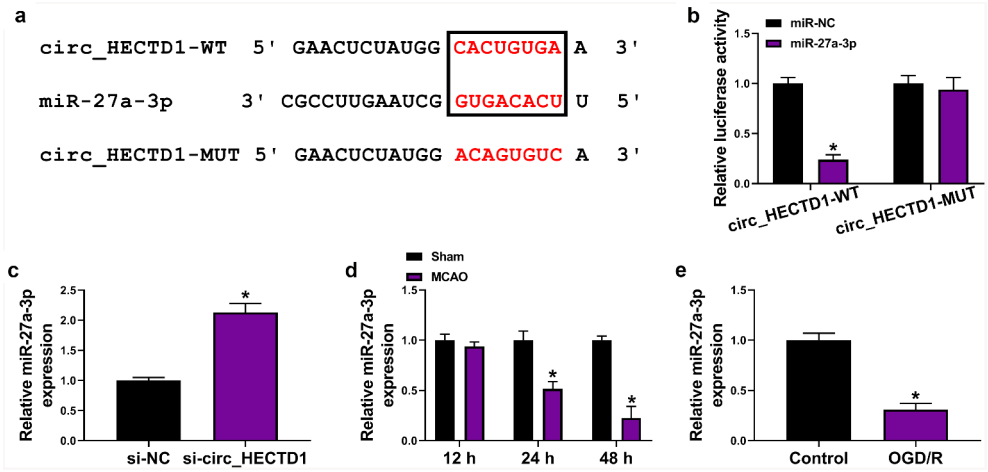

Figure 3. miR-27a-3p was a direct target of circ_HECTD1. (a) Schematic of a putative target sequence for miR-27a-3p in circ_HECTD1 and mutated miR-27a-3p-binding sites. (b) The prediction between circ_HECTD1 and miR-27a-3p was verified by a dual-luciferase reporter assay. (c) miR-27a-3p level was determined in HT22 cells transfected with si-NC or si-circ_HECTD1 by RT-qPCR assay. (d) miR-27a-3p level was measured in mice following MCAO/R at 12, 24, and 48 h by RT-qPCR assay. (e) Relative miR-27a-3p expression was measured in HT22 cells treated with or without OGD/R. *P< 0.05.

control group (Figure 3e), implying the involvement of miR-27a-3p in OGD/R-triggered cell injury *in vitro*. In a word, circ_HECTD1 could bind to miR-27a-3p in HT22 cells.

Circ_HECTD1 deficiency mitigated OGD/R-caused cell damage by interacting with miR-27a-3p *in vitro*

In view of the regulatory role of circ_HECTD1 in miR-27a-3p expression in HT22 cells, whether the effect of circ_HECTD1 on OGD/R-caused cell injury was associated with miR-27a-3p was further probed. First of all, the results of RT-qPCR assay suggested that the co-transfection of anti-miR-27a-3p could counteract the positive role of circ_HECTD1 on miR-27a-3p level in HT22 cells (Figure 4a). Subsequently, functional analysis suggested that si-circ_HECTD1-mediated increase in the number of EdU cells was significantly abolished by miR-27a-3p downregulation in OGD/R-treated HT22 cells (Figure 4b). Similarly, MTT assay also indicated that the reduced expression of miR-27a-3p could abate the acceleration role of circ_HECTD1 silencing on cell proliferation in OGD/R-induced HT22 cells (Figure 4c), accompanied with lowered PCNA level (Figure 4d). Synchronously, the suppressive effect of apoptosis rate caused by circ_HECTD1 downregulation was remarkably relieved by miR-27a-3p inhibitor in OGD/R-triggered HT22 cells (Figure 4e), as described by reduced Bcl-2 level, and elevated Bax and Cleaved PARP levels (figure 4f). All of these results implied that the downregulation of miR-27a-3p could partly reverse the effects of circ_HECTD1 knockdown on proliferation and apoptosis in OGD/R-stimulated HT22 cells.

FSTL1 was a direct target of miR-27a-3p

It has been widely accepted that miRNAs could exert a biological role by targeting mRNAs. Hence, starbase3.0 software was applied to seek the underlying target genes of miR-27a-3p. As presented in Figure 5a, there were some binding sites between miR-27a-3p and FSTL1. Whereafter, the binding relationship was confirmed by a dual-luciferase reporter assay in HT22 cells. Data suggested that the miR-27a-3p upregulation obviously declined the luciferase activity of FSTL1-WT reporter vector but not that of FSTL1-MUT (Figure 5b). Meanwhile, the transfection efficiency of miR-27a-3p mimic or anti-miR-27a-3p was detected and presented in (Figure 5c). And then, the results from RT-qPCR and western blot assay discovered that the manipulation of miR-27a-3p expression could change the mRNA level and protein level of FSTL1, displaying that the overexpression of miR-27a-3p repressed the expression level of FSTL1 and miR-27a-3p downregulation enhanced

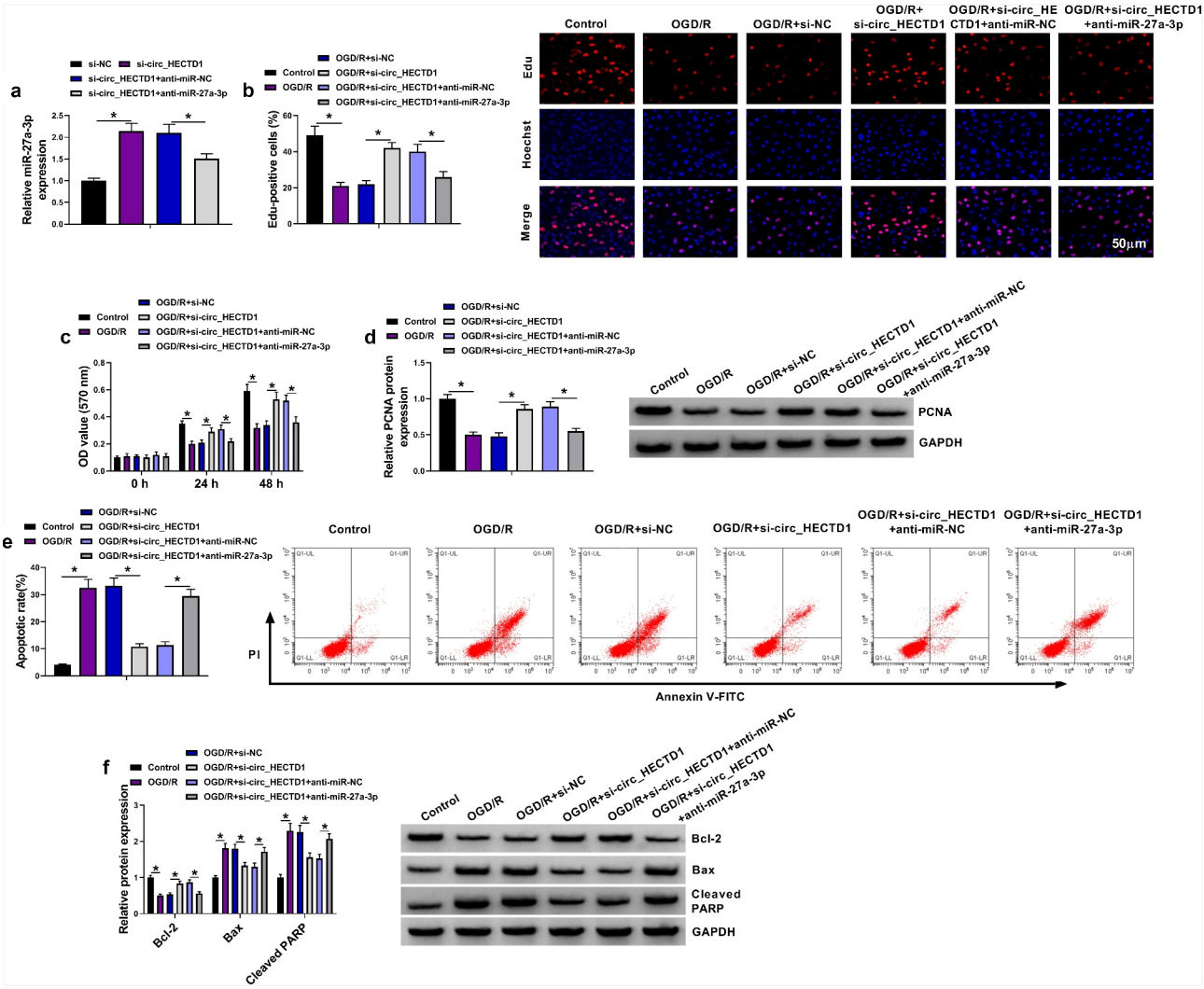

Figure 4. Downregulation of miR-27a-3p reversed the effects of circ_HECTD1 on proliferation and apoptosis in OGD/R-treated HT22 cells. (a) miR-27a-3p level was detected in HT22 cells transfected with si-NC, si-circ_HECTD1, si-circ_HECTD1+ anti-miR-NC, si-circ_HECTD1+ anti-miR-27a-3p by RT-qPCR assay. (b-f) HT22 cells were treated with Control, OGD/R, OGD/R+ si-NC, OGD/R+ si-circ_HECTD1, OGD/R+ si-circ_HECTD1+ anti-miR-NC, OGD/R+ si-circ_HECTD1+ anti-miR-27a-3p. (b) The number of EdU-positive cells was analyzed in treated HT22 cells by EdU incorporation assay. (c) MTT assay was used to assess the proliferative ability in treated HT22 cells. (d) Western blot assay was applied to detect the protein level of PCNA in treated HT22 cells. (e) Flow cytometry assay was performed to analyze the apoptosis rate in treated HT22 cells. (f) Protein levels of Bcl-2, Bax, and cleaved PARP were determined by western blot assay in treated HT22 cells. *P< 0.05.

FSTL1 level in HT22 cells (Figure 5d and 5e). Apart from that, our results suggested that the mRNA level and protein level of FSTL1 were heightened after MCAO/R in a time-dependent manner in mice, indicating the potential role in ischemia *in vivo*. Consistently, we found that the upregulation of FSTL1 in HT22 cells after the treatment of OGD/R versus the corresponding control group (Figure 5h and 5i), suggesting that FSTL1 might take part in OGD/R-induced cell damage *in vitro*. In addition, RT-qPCR and western blot assay exhibited that the introduction of anti-miR-27a-3p could effectively undermine the negative effect of circ_HECTD1 silencing on the mRNA level and protein level of FSTL1 in HT22 cells (Figure 5j and 5k), indicating that circ_HECTD1 could regulate FSTL1 expression by sponging miR-27a-3p. Overall, these data implicated that FSTL1 served as a target of miR-27a-3p.

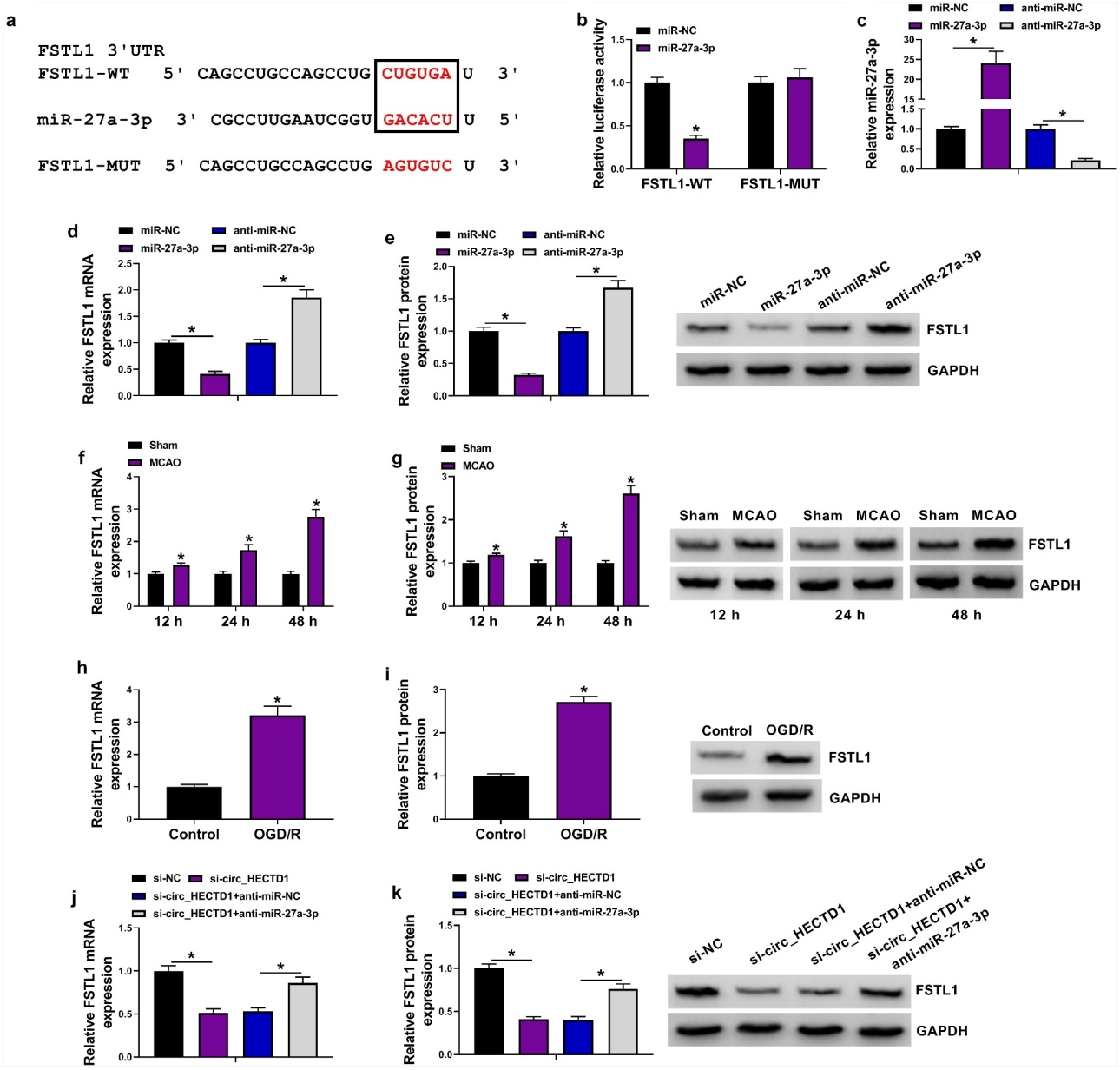

Figure 5. FSTL1 acted as a target of miR-27a-3p. (a) Schematic diagram of the reporter constructs containing the predicted miR-27a-3p-binding site in the3′ UTR of FSTL1. (b) A dual-luciferase reporter assay was employed to verify the binding relationship between miR-27a-3p and FSTL1. (c) miR-27a-3p level was determined in HT22 cells transfected with miR-NC, miR-27a-3p, anti-miR-NC, and anti-miR-27a-3p by RT-qPCR assay. (d and e) relative FSTL1 expression was detected in miR-27a-3p mimic or anti-miR-27a-3p-transfected HT22 cells by RT-qPCR and western blot assays. (f and g) FSTL1 expression was determined in mice following MCAO/R at 12, 24, and 48 h by RT-qPCR assay and western blot assay. (h and i) The mRNA level and protein level of FSTL1 were determined in HT22 cells treated with or without OGD/R by RT-qPCR and western blot assays. (j and k) FSTL1 expression was assessed in HT22 cells transfected with si-NC, si-circ_HECTD1, si-circ_HECTD1+ anti-miR-NC, si-circ_HECTD1+ anti-miR-27a-3p by RT-qPCR and western blot assays. *$P< 0.05$.

miR-27a-3p mitigated OGD/R-triggered cell injury by targeting FSTL1 *in vitro*

Furtherly, we performed rescue assays to explore the influence of miR-27a-3p and FSTL1 on OGD/R-triggered cell injury *in vitro*. As presented in (Figure 6a and 6b), the forced expression of miR-27a-3p markedly decreased FSTL1 expression, which was counteracted by the co-transfection of pcDNA-FSTL1 in HT22 cells. Functionally, cell proliferative ability promoted by miR-27a-3p overexpression was partly reversed by FSTL1 upregulation in OGD/R-treated HT22 cells (Figure 6c and 6d), as evidenced by reduced PCNA level (Figure

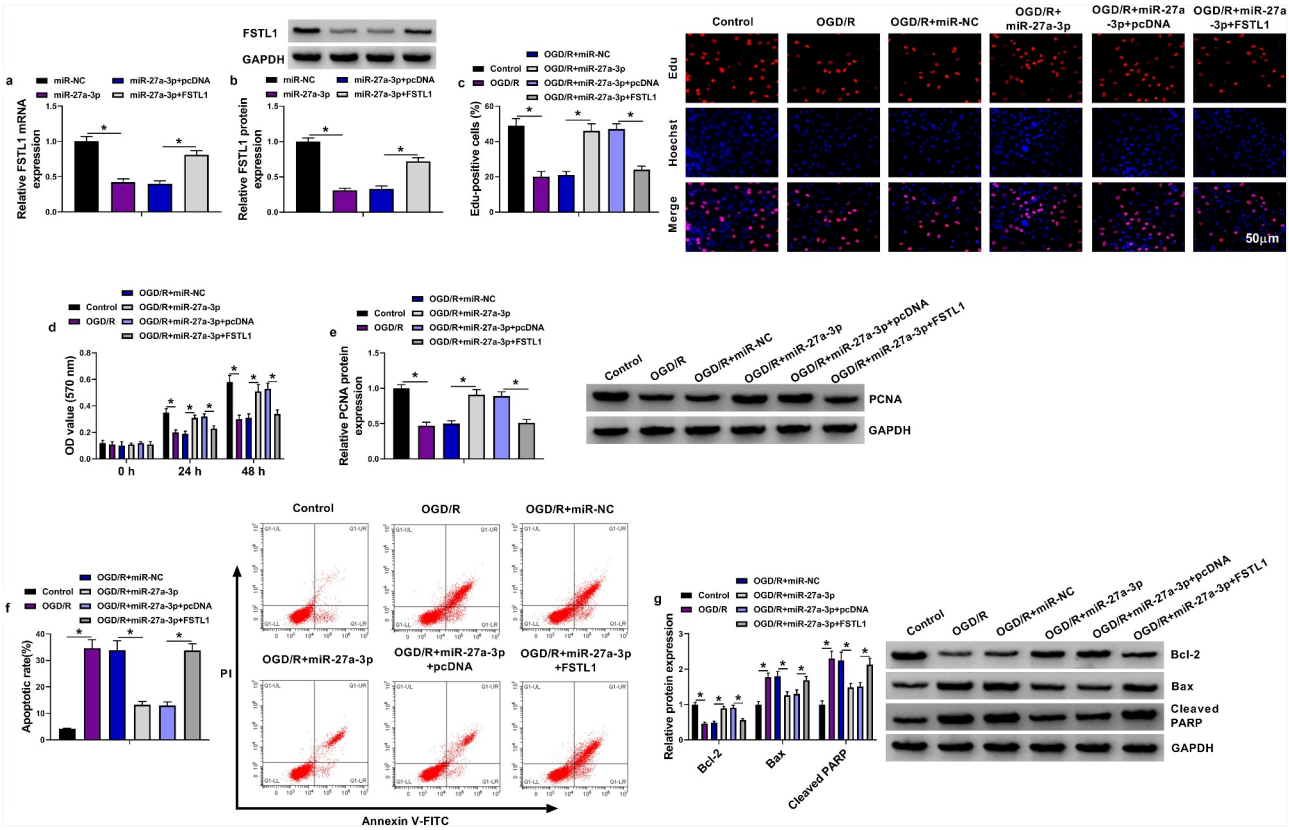

Figure 6. Overexpression of FSTL1 abrogated the effects of miR-27a-3p on proliferation and apoptosis in OGD/R-treated HT22 cells. (a and b) FSTL1 expression was measured in HT22 cells transfected with miR-NC, miR-27a-3p, miR-27a-3p+pcDNA, and miR-27a-3p+FSTL1 by RT-qPCR and western blot assays. (c-g) HT22 cells were treated with Control, OGD/R, OGD/R+ miR-NC, OGD/R + miR-27a-3p, OGD/R+ miR-27a-3p+pcDNA, OGD/R+ miR-27a-3p+FSTL1. (c and d) Cell proliferative ability was assessed in treated HT22 cells by EdU and MTT assays. (e) PCNA protein level was measured in treated HT22 cells by western blot assay. (f) Apoptosis rate was monitored by flow cytometry assay in treated HT22 cells. (F) The assessment of Bcl-2, Bax, and Cleaved PARP protein levels was conducted by western blot assay in treated HT22 cells. *P< 0.05.

6e). In terms of the apoptosis rate, the inhibitory action of apoptosis rate due to the elevated expression miR-27a-3p was notably overturned by pcDNA-FSTL1 in OGD/R-induced HT22 cells (figure 6f), as proved by lower Bcl-2 level, and higher Bax and Cleaved PARP levels (Figure 6g). All of these results implied that FSTL1 overexpression could abolish the suppression of miR-27a-3p on OGD/R-caused cell injury.

Discussion

Nowadays, the biological function and mechanism of circRNAs have been successively identified in mammalian cells by the application of high-throughput sequencing and bioinformatics [23,24]. Plenty of circRNAs have been verified to be an underlying promising attractive biomarker in human diseases owing to the regulatory potency of gene expression and the specificity of molecular structure [25–27]. Intriguingly, it has been widely confirmed that the dysregulation of circRNAs might participate in the regulation of cerebral infarction [28,29]. Recent studies have manifested that irreversible neuronal cell injury was considered a significant feature after cerebral infarction [30–32]. Of note, some reports have indicated that OGD/R-caused cell injury could be applied to explore the progression of cerebral infarction [8,33,34]. In this paper, circ_HECTD1 was identified to be increased in MCAO/R treated brain tissues and OGD/R-triggered HT22 cells, consistent with the form literature [19]. Furthermore, circ_HECTD1 deletion could weaken OGD/R-triggered HT22 cell damage, implying that circ_HECTD1 might take part in cerebral infarction development and an appealing therapeutic target. That was to say, the

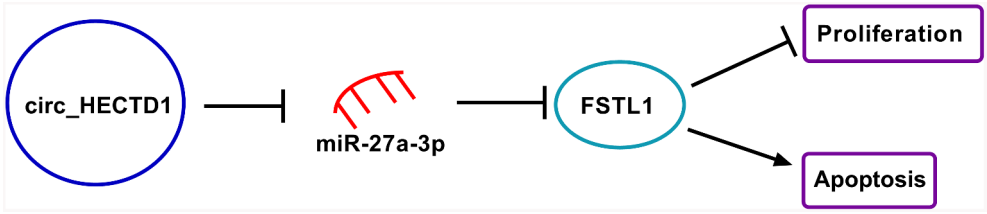

Figure 7. The regulatory role of circ_HECTD1 on HT22 cell proliferation and apoptosis of HT22 cells was mediated by the miR-27a-3p/FSTL1 axis.

downregulation of circ_HECTD1 could exert a neuroprotective effect in cerebral infarction.

Growing evidence discovered that circRNAs performed a variety of biological functions through interacting with miRNAs [13,19]. Moreover, the post-transcriptional regulatory mechanism of circ_HECTD1 was exhibited due to the cytoplasmic expression in HT22 cells. Hence, we further identified the latent circ_HECTD1-interacting miRNAs. The present study verified that circ_HECTD1 could bind with miR-27a-3p. What's more, miR-27a-3p has been documented to be related to cerebral small vessel disease in recent research [35]. Apart from that, miR-27a-3p was previously validated to suppress neuronal apoptosis, infarct volume, and inflammatory response in mice with cerebral ischemia-reperfusion [36]. Therefore, we selected miR-27a-3p for further exploration. In this work, the downregulation of miR-27a-3p was viewed in ischemia-induced injury *in vivo* and *in vitro*, in agreement with a prior report [37]. Besides, the reduced expression of miR-27a-3p could abolish the repression action of circ_HECTD1 knockdown on OGD/R-caused cells injury, verifying the protective role of circ_HECTD1 deficiency in cerebral ischemic damage might be partly ascribed to the interaction with miR-27a-3p.

It has been acknowledged that miRNAs could regulate cerebral ischemic injury through targeting specific mRNAs [38–40]. The present research discovered that the direct target of miR-27a-3p was FSTL1. Meanwhile, previous research suggested that FSTL1, an extracellular glycoprotein, has been confirmed to be involved with cardiovascular diseases and inflammatory diseases [41,42]. In addition, FSTL1 has been pointed out to accelerate neuronal apoptosis and may have the potential for treating ischemic stroke [43,44]. In the work, the upregulation of FSTL1 in ischemia triggered damage *in vivo* and *in vitro* was confirmed for the first time. And the elevated expression of FSTL1 could partially reverse the suppressive action of miR-27a-3p on OGD/R-caused neural cells injury. Furtherly, FSTL1 expression could be modulated by circ_HECTD1/miR-27a-3p in neural cells, supporting the regulatory role of the circ_HECTD1/miR-27a-3p/FSTL1 axis in cerebral infarction (Figure 7).

Conclusions

Taken together, our results discovered that circ_HECTD1 expression was enhanced in OGD/R-treated neural cells. Knockdown of circ_HECTD1 ameliorated OGD/R-induced neural cell damage partly through regulating the miR-27a-3p/FSTL1, providing a crucial preclinical basis for cerebral infarction

Acknowledgments

None

Disclosure statement

No potential conflict of interest was reported by the author(s).

Funding

The authors have no funding to report.

References

[1] Feigin VL, Roth GA, Naghavi M, et al. Global burden of stroke and risk factors in 188 countries, during

1990-2013: a systematic analysis for the global burden of disease study 2013. Lancet Neurol. 2016;15(9):913–924.
[2] Van Middelaar T, Nederkoorn PJ, Van Der Worp HB, et al. Quality of life after surgical decompression for space-occupying middle cerebral artery infarction: systematic review. Int J Stroke. 2015;10(2):170–176.
[3] Koh SH, Park HH. Neurogenesis in Stroke Recovery. Transl Stroke Res. 2017;8(1):3–13.
[4] Miller JB, Merck LH, Wira CR, et al. The advanced reperfusion Era: implications for emergency systems of ischemic stroke care. Ann Emerg Med. 2017;69(2):192–201.
[5] Shibata K, Hashimoto T, Miyazaki T, et al. Thrombolytic therapy for acute ischemic stroke: past and future. Curr Pharm Des. 2019;25(3):242–250.
[6] Cassidy JM, Cramer SC. Spontaneous and Therapeutic-Induced mechanisms of functional recovery after stroke. Transl Stroke Res. 2017;8:33–46.
[7] Sun X, Li X, Ma S, et al. MicroRNA-98-5p ameliorates oxygen-glucose deprivation/reoxygenation (OGD/R)-induced neuronal injury by inhibiting Bach1 and promoting Nrf2/ARE signaling. Biochem Biophys Res Commun. 2018;507(1–4):114–121.
[8] Liang J, Wang Q, Li JQ, et al. Long non-coding RNA MEG3 promotes cerebral ischemia-reperfusion injury through increasing pyroptosis by targeting miR-485/AIM2 axis. Exp Neurol. 2020;325:113139.
[9] Gao Y, Cao X, Zhang X, et al. Brozopine inhibits 15-LOX-2 metabolism pathway after transient focal cerebral ischemia in rats and OGD/R-Induced hypoxia injury in HT22 cells. Front Pharmacol. 2020;11:99.
[10] Kristensen LS, Andersen MS, Stagsted LVW, et al. The biogenesis, biology and characterization of circular RNAs. Nature Reviews. Genetics. 2019;20(675–-691):675–691.
[11] Chen LL. The biogenesis and emerging roles of circular RNAs. Nat Rev Mol Cell Biol. 2016;17(4):205–211.
[12] Greene J, Baird AM, Brady L, et al. Circular RNAs: biogenesis, Function and Role in Human diseases. Front Mol Biosci. 2017;4:38.
[13] Hansen TB, Jensen TI, Clausen BH, et al. Natural RNA circles function as efficient microRNA sponges. Nature. 2013;495(7441):384–388.
[14] Zuo L, Zhang L, Zu J, et al. Circulating circular RNAs as biomarkers for the diagnosis and prediction of outcomes in acute ischemic stroke. Stroke. 2020;51(1):319–323.
[15] Yang J, Chen M, Cao RY, et al. The role of circular RNAs in cerebral ischemic diseases: ischemic stroke and cerebral ischemia/reperfusion injury. Adv Exp Med Biol. 2018;1087:309–325.
[16] Wu F, Han B, Wu S, et al. Circular RNA TLK1 aggravates neuronal injury and neurological deficits after ischemic stroke via miR-335-3p/TIPARP. J Neurosci. 2019;39(37):7369–7393.
[17] Jiang S, Zhao G, Lu J, et al. Silencing of circular RNA ANRIL attenuates oxygen-glucose deprivation and reoxygenation-induced injury in human brain microvascular endothelial cells by sponging miR-622. Biol Res. 2020;53(1):27.
[18] Peng X, Jing P, Chen J, et al. The role of circular RNA HECTD1 expression in disease risk, disease severity, inflammation, and recurrence of acute ischemic stroke. J Clin Lab Anal. 2019;33(7):e22954.
[19] Dai Q, Ma Y, Xu Z, et al. Downregulation of circular RNA HECTD1 induces neuroprotection against ischemic stroke through the microRNA-133b/TRAF3 pathway. In: Life Sci. 2021;264:118626.
[20] Zhang X, Hamblin MH, Yin KJ. Noncoding RNAs and stroke. The Neuroscientist : A Review Journal Bringing Neurobiology, Neurology and Psychiatry. 2019;25(1):22–26.
[21] Han B, Chao J, Yao H. Circular RNA and its mechanisms in disease: from the bench to the clinic. Pharmacol Ther. 2018;187:31–44.
[22] Liu W, Miao Y, Zhang L, et al. MiR-211 protects cerebral ischemia/reperfusion injury by inhibiting cell apoptosis. Bioengineered. 2020; 11(1):189–200
[23] Guo JU, Agarwal V, Guo H, et al. Expanded identification and characterization of mammalian circular RNAs. Genome Biol. 2014;15(7):409.
[24] López-Jiménez E, Rojas AM, Andrés-León E. RNA sequencing and prediction tools for circular RNAs analysis. Adv Exp Med Biol. 2018;1087:17–33.
[25] Memczak S, Jens M, Elefsinioti A, et al. Circular RNAs are a large class of animal RNAs with regulatory potency. Nature. 2013;495(7441):333–338.
[26] Rybak-Wolf A, Stottmeister C, Glažar P, et al. Circular RNAs in the mammalian brain are highly abundant, conserved, and dynamically expressed. Mol Cell. 2015;58(5):870–885.
[27] Ebbesen KK, Hansen TB, Kjems J. Insights into circular RNA biology. RNA Biol. 2017;14(8):1035–1045.
[28] Lu D, Ho ES, Mai H, et al. Identification of Blood Circular RNAs as Potential Biomarkers for Acute Ischemic Stroke. Front Neurosci. 2020;14:81.
[29] Wang SW, Liu Z, Shi ZS. Non-Coding RNA in acute ischemic stroke: mechanisms, biomarkers and therapeutic targets. Cell Transplant. 2018;27(12):1763–1777.
[30] Yuan J. Neuroprotective strategies targeting apoptotic and necrotic cell death for stroke. Apoptosis. 2009;14(4):469–477.
[31] Choi IY, Ju C, Anthony Jalin AM, et al. Activation of cannabinoid CB2 receptor-mediated AMPK/CREB pathway reduces cerebral ischemic injury. Am J Pathol. 2013;182(3):928–939.
[32] Radak D, Katsiki N, Resanovic I, et al. Apoptosis and acute brain ischemia in ischemic stroke. Curr Vasc Pharmacol. 2017;15(2):115–122.
[33] Cao G, Jiang N, Hu Y, et al. Ruscogenin attenuates cerebral Ischemia-Induced Blood-Brain barrier dysfunction by suppressing TXNIP/NLRP3 inflammasome

activation and the MAPK pathway. Int J Mol Sci. 2016;17(9):1418.

[34] Zhan R, Xu K, Pan J, et al. Long noncoding RNA MEG3 mediated angiogenesis after cerebral infarction through regulating p53/NOX4 axis. Biochem Biophys Res Commun. 2017;490(3):700–706.

[35] Yasmeen S, Kaur S, Mirza AH, et al. miRNA-27a-3p and miRNA-222-3p as novel modulators of phosphodiesterase 3a (PDE3A) in Cerebral Microvascular Endothelial Cells. Mol Neurobiol. 2019;56(8):5304–5314.

[36] Zhang E, Chen Q, Wang J, et al. Protective role of microRNA-27a upregulation and HSP90 silencing against cerebral ischemia-reperfusion injury in rats by activating PI3K/AKT/mTOR signaling pathway. Int Immunopharmacol. 2020;86:106635.

[37] Yang T, Wang D, Qu Y, et al. N-hydroxy-N'-(4-butyl-2-methylphenyl)-formamidine attenuates oxygen-glucose deprivation and reoxygenation-induced cerebral ischemia-reperfusion injury via regulation of microRNAs. J Integr Neurosci. 2020;19:303–311.

[38] Bao J, Zhou S, Pan S, et al. Molecular mechanism exploration of ischemic stroke by integrating mRNA and miRNA expression profiles. Clin Lab. 2018;64(04/2018):559–568.

[39] Guo D, Ma J, Yan L, et al. Down-Regulation of Lncrna MALAT1 attenuates neuronal cell death through suppressing beclin1-Dependent autophagy by regulating mir-30a in cerebral ischemic stroke. Cell Physiol Biochem. 2017;43(1):182–194.

[40] Tian YS, Zhong D, Liu QQ, et al. Upregulation of miR-216a exerts neuroprotective effects against ischemic injury through negatively regulating JAK2/STAT3-involved apoptosis and inflammatory pathways. J Neurosurg. 2018;130(3):977–988.

[41] Seki M, Powers JC, Maruyama S, et al. Acute and chronic increases of circulating FSTL1 Normalize energy substrate metabolism in Pacing-Induced heart failure. Circ Heart Fail. 2018;11(1):e004486.

[42] Zhang Z-M, Zhang A-R, Xu M, et al. TLR-4/miRNA-32-5p/FSTL1 signaling regulates mycobacterial survival and inflammatory responses in Mycobacterium tuberculosis -infected macrophages. Exp Cell Res. 2017;352(2):313–321.

[43] Liu YP, Ju ML, Yu FQ. Clinical significance of FSTL 1, Bax, Bcl-2 in acute cerebral infarction and its relationship with hemorrhagic transformation. Eur Rev Med Pharmacol Sci. 2020;24(16):8447–8457.

[44] Liang X, Hu Q, Li B, et al. Follistatin-like 1 attenuates apoptosis via disco-interacting protein 2 homolog A/Akt pathway after middle cerebral artery occlusion in rats. Stroke. 2014;45(10):3048–3054.